Available online at www.sciencedirect.com
SCIENCE DIRECT®
Journal of Hydrology 273 (2003) 205–216
Journal of Hydrology
www.elsevier.com/locate/jhydrol

# The use of stream flow routing for direct channel precipitation with isotopically-based hydrograph separations: the role of new water in stormflow generation

Carl E. Renshaw*, Xiahong Feng, Kelsey J. Sinclair, Raymond H. Dums

*Department of Earth Sciences, Dartmouth College, Hanover, NH 03755, USA*

Received 14 December 2001; revised 18 November 2002; accepted 22 November 2002

**Abstract**

Understanding the pathways by which event water contributes to stream stormflow provides insight into stormflow generation mechanisms. We analyze the impact of storm size on the relative contribution of event water to stormflow by using natural variations in the oxygen isotopic composition of precipitation and stream water to separate multiple stormflow hydrographs from a single fourth-order, 1212 ha catchment. We extend previous isotope-based hydrograph separations by independently accounting for the contribution of event water via direct channel precipitation to the stream hydrograph. The direct channel precipitation contribution is determined using a numerical model of stream flow routing though the catchment, taking precipitation and digital elevation data as input variables. For the range of storm sizes sampled, having recurrence intervals ranging from less than a week to ~4 months, essentially all the event water in stream stormflow can be attributed to direct channel precipitation. Event water not directly falling on the stream channel indirectly contributes to stormflow by increasing the subsurface discharge of pre-event water to the stream. Neither the hydrograph separation data, field observations during the precipitation events, nor experimental observations of flow in a large-scale natural soil column extracted from the watershed are consistent with macropore flow or groundwater ridging as the primary mechanism responsible for increasing subsurface discharge. Results from a series of artificial rain experiments using the unsaturated natural soil column are consistent with a preferential kinematic flow model and indicate that the discharge of pre-event water to the stream during a storm event may be controlled by kinematic flow processes within the watershed soils.


*Keywords:* Hydrographs; Streamflow routing; Kinematic waves; Hydrograph separation

## 1. Introduction

Understanding the flow of water and transport of contaminants through watersheds is essential for accurate analyses of many environmental problems, including the long-term acidification of surface and subsurface waters, sensitivity of aquatic biota to episodic pulses of acidified waters associated with large runoff events, impact of land use on riparian ecosystems, the transport of pollutants from non-point sources, and how ecosystems respond to perturbations such as changes in climate. By regulating residence times and the degree of water–rock interaction, flow

* Corresponding author. Tel.: +1-603-646-3365; fax: +1-603-646-3922.
*E-mail address:* carl.e.renshaw@dartmouth.edu (C.E. Renshaw).

0022-1694/03/$ - see front matter © 2003 Elsevier Science B.V. All rights reserved.
PII: S0022-1694(02)00392-X

and transport also directly impact many geochemical, geomorphological, and ecological processes (e.g. Clow and Sueker, 2000; Kirchner et al., 2000; Langmuir, 1997; Mullholland, 1993; Schnoor, 1996).

Precipitation reaches a stream through one of three basic pathways; (1) by falling directly on the stream channel, (2) via overland flow on either saturated soils or surfaces with low infiltration capacities, or (3) via subsurface flow pathways. The importance of subsurface flow pathways in the generation of stream stormflow in forested catchments has long been recognized (Hursch, 1936). While saturation overland flow (Horton, 1933) can be a significant runoff-generating mechanism locally (Beston, 1964; Dunne and Black, 1970), and while successful predictions of stormflow hydrographs can be obtained using models conceptually based on saturation overland flow as the dominant runoff-generating mechanism (Hoggon, 1997), subsurface flow is usually the dominant mechanism of streamflow generation in forested, temperate catchments (Freeze, 1974; Genereux and Hooper, 1998; Torres et al., 1998).

Quantitative evidence for the importance of subsurface flow in stormflow generation comes from numerous studies that have used oxygen and hydrogen isotopic variations in natural precipitation to separate stream hydrographs into pre-event or 'old' water, and event or 'new' water contributions. In a recent summary of isotopically-based hydrograph separation studies within a large range in catchment areas (Genereux and Hooper, 1998), the average percent old water at peak discharge is 70 ± 20%. The data for the contribution of pre-event water to the event hydrograph have a similar mean standard deviation. Similar conclusions have been reached in studies using chemically-based hydrograph separations (Hooper et al., 1990).

It follows that approximately one third of the precipitation falling on a watershed ends up in the stream almost immediately and thus has a very short residence time in the catchment. While not the dominant source of water to the stream, understanding the short residence time component of stream discharge is important for many problems as this water does not interact extensively with the chemically and biologically active watershed soils. For example, some short residence time pathways, such as direct channel precipitation, allow acidified precipitation to reach a stream without being buffered. Others, such as saturation overland flow or subsurface macropore flow, allow for limited soil–water interactions which may be sufficient to buffer the acidified precipitation. Thus, there is a need to understand not only the total fraction of new water in the stream, but also what part of that fraction reaches the stream via direct channel precipitation versus other off-channel pathways such as saturation overland flow or subsurface macropore flow. While several investigators have used isotopic and chemical tracers to sub-divide the old water contribution to a stream into different end-member components (e.g. groundwater versus soil water, Bazemore et al., 1994; Sueker et al., 2000), less attention has been directed toward quantifying the relative contributions of different sources of new water to a stream.

Complicating the analysis of the new water component of stream discharge is the significant variability between, and within, catchments in the new water contribution to a stream. The lack of a distinct correlation between the relative contributions of new and old water contributions and catchment size (Genereux and Hooper, 1998) suggests that other factors, such as the amount and intensity of precipitation, soil depth variability (Ross et al., 1994), soil composition and structure (Beven and Germann, 1982; McDonnell, 1990; Mulholland et al., 1990), antecedent moisture conditions (Elsenbeer et al., 1994), and underlying bedrock topography (Brammer and McDonnell, 1996), significantly affect the relative contributions of different flow pathways to an event hydrograph.

To define better the factors affecting the relative contributions of new and old water to a stream, we seek to quantify the relative contributions of old and new water as a function of the magnitude of the precipitation event. These contributions are quantified using natural variations in the oxygen isotopic composition of precipitation and of stream water to separate multiple stormflow hydrographs from a single catchment (Mink Brook, NH). We extend previous isotope-based hydrograph separation analyses by independently accounting for the contribution of new water via direct channel precipitation to the stream hydrograph using a numerical model of stream flow routing of direct channel precipitation through the catchment. We also directly observe

vertical subsurface flow of water and tracer through Mink Brook soil using a large-scale (~0.5 m) soil column extracted from the Mink Brook watershed. These experiments suggest that flow mechanisms within the unsaturated zone of Mink Brook are an important control on the timing and magnitude of runoff generation in the Mink Brook catchment.

## 2. Study area

Precipitation and stream discharge sampling was performed in the Mink Brook watershed near Etna, NH, USA (43° 42′ N and 72° 12′ W). This study focuses on the upper 12.12 $km^2$ of the catchment. The sampling site (Fig. 1) was selected for its proximity to a USGS gauging station that recorded stream discharge until 1997. Above the gauging station, the terrain is hilly and steep, with an average stream gradient of 0.018. The total change in elevation from headwaters to the gauging station is ~300 m.

Average monthly precipitation is 7.9 cm/month and is approximately uniformly distributed throughout the year. The site receives ~25% of its precipitation in the form of snow. Water samples were collected after spring runoff in the summer and early fall of 1998, 1999 and 2000.

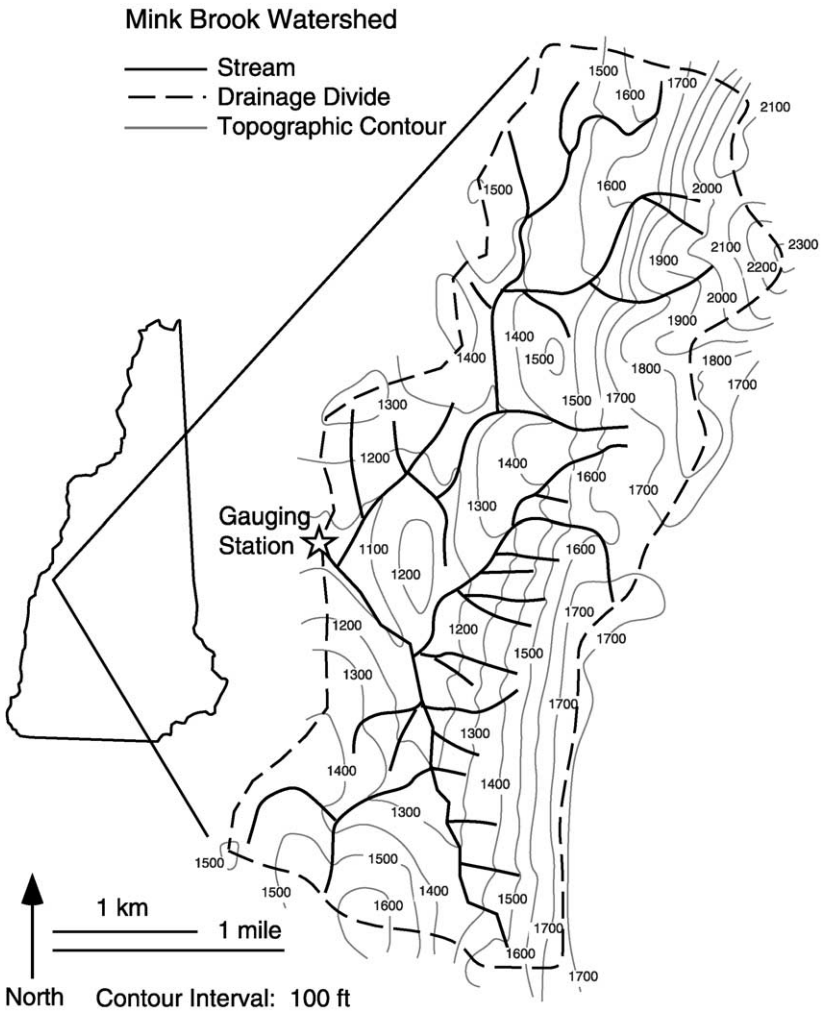


Fig. 1. The Mink Brook Catchment.

Land use in the upper portion of the catchment is approximately 90% forested and 10% pasture and residential land. The bedrock consists of Ordivician Amonusuc metavolcanics and metasediments. The general soil cover consists of a 5–10 cm thick O horizon grading into the A horizon. At a depth of 20–30 cm, the A horizon overlays a dark gray silty B layer a few tens of centimeters thick. Typically, at a depth of 50 cm, a ~5 cm saprolitic Cr horizon grades into bedrock regolith.

## 3. Methods

Biweekly baseflow, groundwater, and precipitation samples were collected between May, 1998 and October, 2000 to quantify seasonal variations in isotopic compositions. Stream samples were collected at the USGS gauging station. Groundwater was sampled using a shallow piezometer located 10 m upstream from the gauging station. The piezometer was screened just above the top of the weathered bedrock at a depth of ~50 cm. Precipitation samples were collected at the Dartmouth College Observatory, 11 km west of the gauging station. In addition, more intense water sampling was conducted during isolated storm events. Sampling began just prior to the onset of precipitation and continued throughout the storm and the following several days until the stage of the stream returned to pre-storm levels. During storm events, rain samples were collected in a clearing adjacent to the gauging station. Storm events were sampled during the summer and early fall when the isotopic composition of rainwater is usually significantly different (>1‰) than that of stream baseflow.

Stream water was collected manually and with the assistance of an auto sampler. Pressure transducers and data loggers were used to monitor the stream stage every 15–30 min. Stage values were converted to stream discharge using a rating curve established by the USGS for the Mink Brook gauging station. Total storm precipitation near the gauge was measured manually using a plastic rain gauge. Precipitation was also recorded in increments of 0.1″ with an automated rain gauge. Unfortunately, many of the automated readings were lost due to instrument damage.

All samples were filtered into polyethelyne bottles using 0.45 μ filters attached to 50 ml syringes. Selected samples were analyzed for $^{18}O$ using the method of $CO_2$ equilibration (IAEA, 1981). The $^{18}O/^{16}O$ ratio was determined using an isotope ratio mass spectrometer, and results expressed in the $\delta$ notation as parts per thousand difference relative to Vienna Standard Mean Ocean Water (VSMOW). The precision of the $\delta^{18}O$ measurements is 0.1‰ ($1\sigma$).

The soil column was extracted from a forested site ~5 km downstream from the gauging station. Although obtained outside the upper portion of the catchment used for the flow studies, the soil column was collected at a site having similar podzol soil, bedrock, topography, and forest cover as the upper portion of the catchment. The column was collected by sliding a 25 cm diameter PVC tube over the soil core as the edges of the core where dug away. The column was separated from its base using a steel plate. The soil column extended down to the soil/weathered saprolite contact (0.48 m). Great care was taken to minimize the disruption or destruction of any macropores in the column during collection. Prior to testing, the column was stored in a cold room at 2 °C. The volume weighted average porosity of the column was 55%, as determined from separate soil samples collected after the column was extracted.

To prepare the column for flow and tracer experiments, four equally-spaced 5 mm diameter holes were drilled into the column at each of three equally spaced depths. A Rhizon soil moisture tensiometer was inserted through each hole and ~2 cm into the soil. The open end of each tensiometer was attached to a 7.5 ml vaccutainer tube. A constant suction was maintained in each tube by attaching each tube to a vacuum pump drawing 0.17 MPa.

A series of artificial rain experiments were performed. During each experiment, artificial rain containing 60 ppm chloride tracer was applied to the top of the column at a rate of 3.13 cm/hr for 40 min. A total of nine experiments were performed. The column was allowed to drain completely prior to beginning each experiment. Rainfall was simulated using the method of Ogden et al. (1997). The base of the column was divided into four separate, equally-sized quadrants and effluent from each quadrant collected in 30 ml increments. Chloride concentrations in the column effluent were determined using an ion chromatograph, an ion specific electrode, or calibrated total dissolved solids (TDS) meter.

Random samples from throughout the experiment were analyzed using both the TDS meter and ion chromatograph to ensure an accurate calibration of the TDS meter and that increases in TDS readings were primarily due to increasing chloride concentrations.

The volume and chloride concentration of soil water collected in each vacutainer were sampled at the end of each experiment. Each vacutainer was then replaced prior to beginning the next experiment. Chloride concentrations for all vacutainer samples were analyzed using an ion chromatograph.

## 4. Results

The $\delta^{18}O$ values of rain and baseflow were used in a two component mixing model to separate the total discharge into the proportions of new and old water using the mass balance equation:

$$Q_o = \left[ \frac{(\delta^{18}O_s - \delta^{18}O_r)}{(\delta^{18}O_b - \delta^{18}O_r)} \right] Q_s \quad (1)$$

where $Q$ is discharge and the subscripts o, s, r, and b indicate old, stream, rain, and baseflow components, respectively. As groundwater samples generally yielded $\delta^{18}O$ values $\sim 1.0‰$ lower than baseflow, using the isotopic composition of groundwater as the old water end member results in an over-estimation of the proportion of new water (Jenkins et al., 1994). Thus, the isotopic composition of stream baseflow samples taken just prior to the onset of precipitation was used as the baseflow end member. Precipitation end member $\delta^{18}O$ values were determined using the incremental mean approach (McDonnell et al., 1990) over the duration of the storm to incorporate temporal variations in the isotopic composition of the rain.

A total of 11 precipitation events ranging in size from 2 to 33 mm were sampled. These sizes correspond to storms having recurrence intervals ranging from a few days to approximately ~4 months. The proportion of the total stream discharge at peak flow composed of old water ranged from 74 to 92%, with an average of 84%. These results are similar to those determined in previous studies (Genereux and Hooper, 1998).

The effluent discharge from the base of the column, normalized by the input flux, for the first flow and tracer experiment is shown in Fig. 2. While water consistently began to discharge from the base of the column ~20 min after the start of the rain application, the chloride tracer did not appear at the base of the column until after the fifth application, i.e. breakthrough of the chloride tracer took an order of magnitude longer than the time required to activate flow at the base of the column. The total volume of water added to the column at the end of the fifth application, when the chloride first appeared, was approximately 40% of the total pore volume of the column.

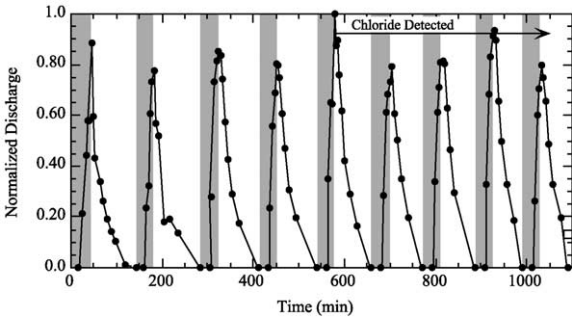


Fig. 2. Discharge from the base of the soil column, normalized by the rainfall rate of 3.13 cm/hr. Shaded regions indicate times during which rainfall was applied to the top of the column. Notice that while discharge at the base of the unsaturated column increases approximately 20 min after the start of rainfall, chloride tracer in the rain did not appear until after the fifth rainfall event.

## 5. Discussion

### 5.1. Contribution of new water to storm discharge

When the data for the sampled storms are plotted as a function of storm size, the percent old water at peak discharge is positively correlated ($r^2 = 0.87$) with storm size (Fig. 3). Essentially similar results are obtained if only the additional discharge due to the event is considered, i.e. the stream discharge minus the pre-event baseflow. This correlation reflects changes in the relative contributions of different flow paths to stream discharge as a function of storm size. Additional insight into this change in new water contribution is obtained from a more detailed analysis of the new water hydrograph.

New water may contribute to stream discharge either by direct precipitation on the stream channel or

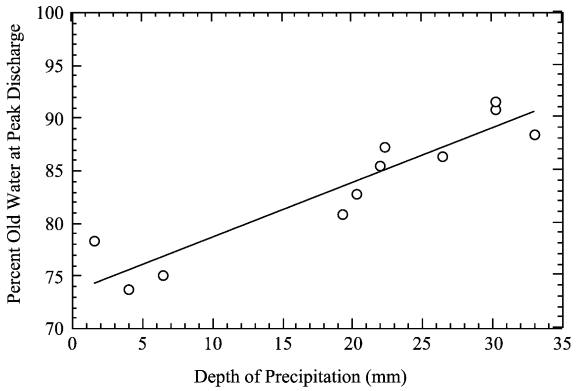


Fig. 3. Percent of total stream discharge composed of old water at peak discharge versus size of precipitation event.

by runoff from off-channel sources. Overland flow was not observed during runoff conditions at this site; however, new water may reach the channel through subsurface quickflow, particularly if preferential flow pathways such as macropores are active. While new water runoff via subsurface flow paths is difficult to quantify, the contribution of direct channel precipitation to the event hydrograph can be explicitly modeled using well established methods for routing flow through a stream network.

Models for routing stream flow through a network of channels are based on continuity, which requires that the gradient in stream discharge $\partial Q/\partial x$ along the direction of flow equal

$$\frac{\partial Q}{\partial x} = q - \frac{\partial A}{\partial t} \tag{2}$$

where $A$ is the cross sectional area of the flowing channel perpendicular to flow, $t$ is time, and $q$ is the lateral inflow per unit length of channel due to baseflow, runoff, and direct channel precipitation. In kinematic flow models, it is assumed that there is a one-to-one correspondence between stream stage and discharge of the form (Eagleson, 1970)

$$Q = \alpha A^m \tag{3}$$

For example, using Manning's equation and assuming a wide, rectangular channel of width $w$, $m = 5/3$ and (Bras, 1990)

$$\alpha = \frac{1}{n}\frac{S^{1/2}}{w^{2/3}} \tag{4}$$

where $S$ is the channel slope and $n$ is the Manning roughness coefficient.

Combining Eqs. (2) and (3) yields the governing equation for kinematic flow routing

$$\frac{\partial A}{\partial t} + \alpha\frac{\partial A^m}{\partial x} = q \tag{5}$$

Eq. (5) can be solved numerically using an explicit finite difference approximation (Bras, 1990). This numerical scheme is consistent, convergent, and stable subject to the condition

$$\alpha m A^{m-1}\frac{\Delta t}{\Delta x} \leq 1 \tag{6}$$

For all simulations we used an initial time step $\Delta t = 10$ s. The stream network shown in Fig. 1 was discretized by first placing nodes at the head of each first-order stream, at each confluence of two channels, and at the basin outlet at the gauging station. The change in drainage area between each pair of adjacent nodes was then determined and an additional node placed at the mid-point of the reach having the largest change in drainage area. Additional nodes were similarly added as long as the stability criterion was satisfied. The final discretization of the stream network contained 434 nodes. During the simulation of each storm, changing values for $A$ required that the time step be decreased to maintain stability.

Prior to simulating each storm, steady-state baseflow was routed through the catchment by assuming that the baseflow entering the stream along each reach between two adjacent nodes is proportional to the change in catchment drainage area along the reach. The baseflow flux per unit drainage area $q_o$ was determined by dividing the stream discharge at the gauging station prior to the onset of precipitation by the catchment drainage area (12.12 km$^2$). The baseflow was held constant at its pre-storm value during the simulation of storm flow.

All stream channels are assumed to have a rectangular cross section. We calculate the width $w$ of the channel at each node using the standard hydraulic geometry relation

$$w = a_1 Q^b \tag{7}$$

where $b$ is an empirical constant $\sim 0.5$ (Dunne and Leopold, 1978). In the eastern US, average stream discharge is linearly related to drainage area $D$ (Dunne

and Leopold, 1978), allowing Eq. (7) to be written

$$w = a_2 D^b \tag{8}$$

The value of the constant $a_2$ is determined from the width of Mink Brook at the gauging station (7 m).

Stream discharge and slope measurements near the gauging station indicate a value of Manning's $n$ for Mink Brook ~0.045. This value is consistent with the range of values (0.040–0.050) expected for a mountain streams with rocky beds composed of gravel, cobbles, and a few boulders (McCuen, 1998).

Although an automatic rain gauge was used to measure variations in rainfall intensity during storms, instrument damage resulted in the loss of most of these data. Total depth of precipitation for each storm was measured independently. Field observations during sample collection indicate that within the resolution of the stream discharge measurements (15–30 min), the starting and ending times for each storm can be closely approximated by the first increase in stream discharge above its pre-storm baseflow and the peak stream discharge (Fig. 4). Hence, for each storm, rainfall intensity is assumed to be constant throughout the entire storm, beginning with the first measured increase in stream discharge above pre-storm baseflow and ending at peak discharge. The rainfall intensity $I$ is calculated as the total depth of precipitation for a given storm divided by the time between the initial increase in discharge and peak discharge. The lateral inflow to the stream during the precipitation event is then given as

$$q = \frac{\Delta D}{\Delta x} q_o + WI \tag{9}$$

where $\Delta D$ is the change in drainage area along a reach between two adjacent nodes separated by a distance $\Delta x$. For the storms considered here, the rainfall intensity $I$ was typically two to three orders of magnitude greater than the pre-storm baseflow flux $q_o$. The rainfall intensity is set to zero after the observed peak discharge.

The channel slope along each reach was determined from USGS digital elevation data (DEM) for the Mink Brook watershed. The DEM had a spatial resolution of 30 m. The DEM was analyzed and the channel network extracted, including the along channel slopes, using Rivertools™ software.

Fig. 5(a) and (b) show, for two of the sampled storms, the observed discharge hydrographs along with the component of the simulated hydrograph representing the routing of the direct channel precipitation past the gauging station. Also shown on each graph is the discharge of new water calculated using isotope-based hydrograph separation. The simulated direct-channel precipitation hydrographs closely agree with the discharge of new water determined isotopically. Similar results were found for the other sampled storms. These results are summarized in Fig. 5(c) which compares the modeled total volume of water falling directly on the stream channel during a storm to the observed volume of new

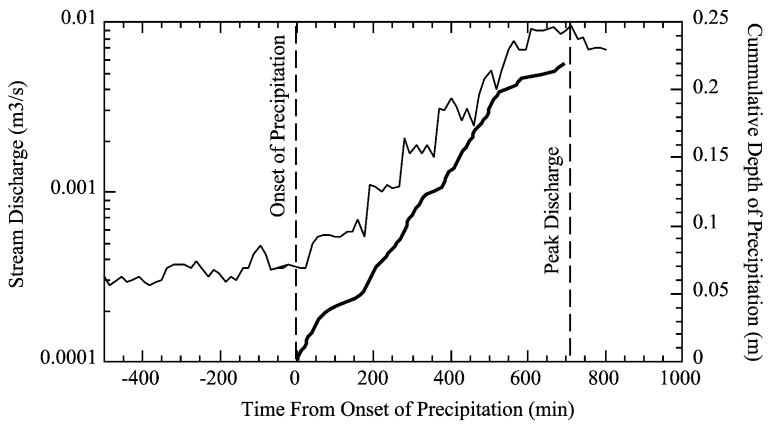


Fig. 4. Stream discharge and cummulative depth of precipitation (bold line) for the storm on October 6, 2000. Increase in stream discharge and peak discharge closely follow the onset and end of precipitation.

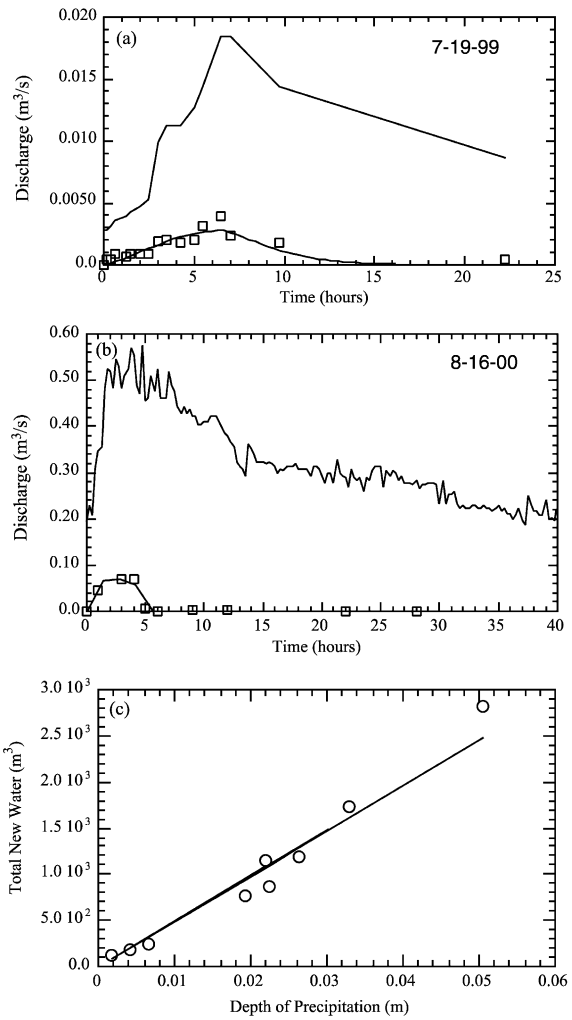


Fig. 5. Upper curves in a and b are observed stream discharge. Symbols represent component of total discharge composed of new water as determined via isotopically-based hydrograph separation. Lower curves in a and b are the component of the simulated hydrograph derived from direct channel precipitation. Predicted total volume of direct channel precipitation from the stream flow routing model (line) versus volume of new water determined isotopically (circles) is shown in c.

water in the stream during the event, as determined isotopically. The close agreement shown in these figures is surprising given the assumptions of the simple stream flow routing model used. While a detailed sensitivity analysis of the model is beyond the scope of this work, some preliminary work suggests that the results of the simulation are robust. For example, while field observations indicate that assuming a rectangular channel geometry is appropriate, essentially similar results are obtained assuming a triangular geometry. Nor are the results highly sensitive to Manning's $n$, at least over the range typical of streams similar to Mink Brook ($\sim$0.040–0.050, McCuen, 1998). The results from these simulations consistently indicate that the new water contribution to the event hydrograph is almost entirely due to direct channel precipitation and that saturation overland flow and/or rapid subsurface preferential flow are not significant sources of new water to the stream. For the range of precipitation events considered here (having recurrence intervals ranging from less than a week to $\sim$4 months), all precipitation falling on the watershed, other than that directly falling on a stream channel, remains stored in the watershed for a period of time significantly longer than the time scale of a single precipitation event.

### 5.2. Generation of storm hydrographs

While precipitation not falling on the stream channel does not directly contribute to stream discharge during a storm event, it does exert an important control on the generation of runoff to the stream. Fig. 4 shows that the increase in stream discharge is temporally related to the precipitation event; stream discharge begins to increase $\sim$30 min after the onset of precipitation and peak discharge occurs $\sim$20 min after the precipitation ends. The difference between the simulated hydrograph and the observed increase in total stream discharge above its pre-event baseflow represents the additional contribution of off-channel sources (i.e. surface and subsurface runoff) to stream discharge. As saturation overland flow and/or rapid subsurface preferential flow are not significant sources of water to the stream, the additional contribution of off-channel sources represents an increase in old water delivered to the stream via subsurface flow. Interestingly, even small amounts of precipitation over the watershed (a few millimeters) significantly increase subsurface flow over the time scale of the event.

As the water table in the Mink Brook catchment is typically at a depth of half a meter or more, to activate additional subsurface flow to the stream, any precipitation must increase fluid pressures at the base of

the unsaturated zone over a relatively short time scale (i.e. a few tens of minutes). Torres et al. (1998) reached a similar conclusion based on their observations in a steep, headwater basin in the Oregon Coast Range. Two flow mechanisms are commonly invoked to explain the rapid increase in fluid pressure at the base of the unsaturated zone and subsequent increase in baseflow to the stream; macropore and kinematic or 'translatory' flow (Beven, 1989).

Macropore flow occurs when soil structures, root casts, fractures, etc. serve as conduits for rapid fluid flow along these preferential flow pathways (Beven and Germann, 1982). Hill-slope runoff studies (McDonnell et al., 1990) indicate that preferential flow pathways significantly affect subsurface flow in the saturated zones of a catchment. However, large macropores often hinder or decrease flow in unsaturated soils as they drain easily, significantly decreasing their relative permeability (Brown et al., 1999). Neither our hydrograph separations nor our column studies provide evidence for the rapid (i.e. over the time scale required for the stream discharge to increase after a precipitation event begins) transmission of event water through the subsurface, as might be expected if macropores were active.

The term 'translatory flow' is an operational definition coined by Hewlett and Hibbert (1967) to describe the phenomenon by which water infiltrating into the top of a column of partially-saturated porous material displaces fluid at lower depths and results in outflow from the base of the column long before the infiltrated water reaches the bottom of the column. Kinematic flow is a specific physical mechanism that can cause translatory flow. If the water content of the soil is near that required for fluid flow (i.e. near the retention capacity), then only a small volume of additional water is required to activate flow and transmit a wave of increased fluid pressure through the system (Charbeneau, 1984). The kinematic flow model is similar to the conceptual pressure wave propagation model described by Torres et al. (1998) based on their observations of the response of a steep, headwater basin to an artificial rain event.

The results from the artificial rain experiments using the natural soil column demonstrate the ability of Mink Brook soil to transmit pressure waves quickly to the base of the unsaturated zone (Fig. 2). In these experiments, flow from the base of the 0.48 m long unsaturated column appeared ~20 min after the onset of artificial rain to the top of the column. However, chloride tracer within the applied rain was not detected at the base of the column until after more than 200 min of total precipitation.

The propagation of a pressure wave through unsaturated porous media can be quantified using a model similar to that used for routing stream flow through a channel network. In stream flow routing, the kinematic constitutive relationship between discharge and storage is as given in Eq. (3). The equivalent kinematic constitutive relation for gravity-dominated flow through unsaturated media is a modified form of the Brooks-Corey (Tindall and Kunkel, 1999) model (Charbeneau, 1984; Colbeck, 1972)

$$q = K\left(\frac{S - S_r}{1 - S_r}\right)^n \tag{10}$$

where $q$ is the specific discharge, $K$ is the saturated hydraulic conductivity and $n$ is an empirical material constant. The term in the brackets is the effective water saturation, which is a function of the total $S$ and residual $S_r$ saturations. Here total saturation is defined as the water content divided by the pore volume and residual saturation is the retention capacity divided by pore volume. We assume that the porous medium is homogeneous with an initial uniform saturation $S = S_r$. At $t = 0$, the onset of precipitation increases the saturation at the top of the column by an amount $\Delta S$. Steady state infiltration of the rainfall maintains the saturation at the surface $S = S_r + \Delta S$. Combining the constitutive relation with conservation of mass for one dimensional vertical flow gives the propagation velocity of the pressure wave $v_p$ as (Hibberd, 1984)

$$v_p = \frac{q}{\phi}\frac{S_r}{\Delta S} \tag{11}$$

where $\phi$ is the porosity.

In our soil column experiments, the velocity of the pressure wave is determined from the difference in time between the onset of precipitation and the first discharge of water from the base of the column (~20 min). We assume that since the column is completely drained prior to beginning each experiment, the initial water content of the column is equal to the retention capacity. We hypothesize that due to hysteretic effects in the wetting and drainage of unsaturated media (Freeze and Cherry, 1979),

the retention capacity increases slightly between consecutive experiments as small, poorly draining pores are increasingly saturated. However, we hypothesize that the change in water content needed to propagate the pressure wave $\Delta S$, which we conceptualize as the water needed to fill the larger, easily drained pores, remains constant between experiments. Hence, from Eq. (9), as the residual saturation increases, so too does the wave propagation velocity. This is consistent with the trend of our observed wave propagation velocities (Fig. 6). A best fit curve of the form of Eq. (9) to the data yields $\Delta S = 0.067$. Alternatively, it may be that $S_r$ is constant and $\Delta S$ decreases between experiments. However, we find this hypothesis conceptually more difficult to justify.

Interestingly, the average observed propagation time for the wave through the soil column (~20 min) is generally consistent with the time required for the stream discharge to increase following the onset of precipitation (~30 min). We caution that it is uncertain to what degree the results from a single soil column study can be extrapolated to the entire heterogeneous catchment. However, the existence of kinematic flow in the unsaturated zone is also consistent with the magnitude of the increase in stream discharge generated by each storm. We calculate the flood discharge of an event by subtracting the pre-event baseflow from the event hydrograph and integrating over the duration of the event (from the onset of precipitation until the stream discharge returns to its pre-event value). The flood discharge is then normalized by the volume of precipitation falling on the watershed during the event. This normalized flood discharge is plotted versus the number of days since the last rainfall in Fig. 7. Notice that when the time since the last rainfall is short, the flood discharge is high relative to the volume of rain falling on the catchment. However, if more than a few days pass between precipitation events, then the flood discharge is nearly a constant fraction of the precipitation volume. Similar variations are not observed for normalized flood discharge versus size of the precipitation event.

The higher normalized flood discharges when the time between precipitation events is short may reflect differences in the size of the catchment area where the ground water is shallow enough to respond rapidly to the pressure wave; recharge from recent precipitation events raises ground water levels and results in a greater area of the catchment having shallow depths to ground water. However, while not necessarily conclusive given the heterogeneity of the catchment, we find no correlation between the normalized flood discharge and the height of the water table recorded in the shallow piezometer prior to the onset of the precipitation. As an alternative hypothesis, we suggest that when the time between precipitation events is short, the

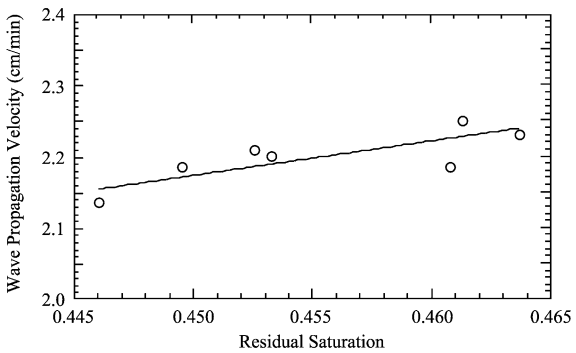


Fig. 6. Observed propagation velocity of the fluid pressure wave through the soil column versus initial saturation of the column. Line is the least squares best fit to the data of a model of the form of Eq. (9).

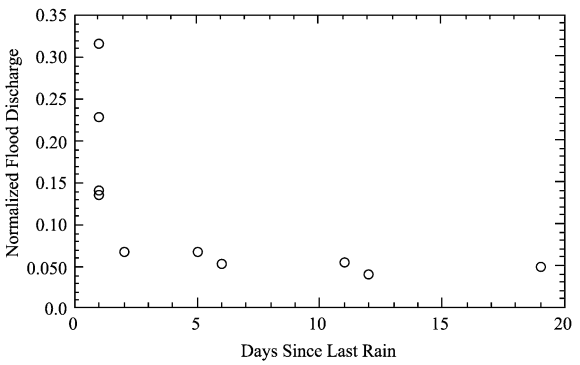


Fig. 7. Normalized flood discharge versus days since last rainfall. Flood discharge represents the integrated event hydrograph minus pre-event baseflow. Flood discharge is normalized by the volume of precipitation falling on the watershed during the event.

soil water content is near the residual saturation and the fluid pressure wave generated by the rain is more efficiently conducted to the base of the saturated zone, regardless of the depth to the water table. However, after a few dry days, the water content decreases due to evapotranspiration, slowing the transmission of the pressure wave and reducing the normalized flood discharge.

## 6. Conclusions

Our results suggest that, for the range of storm sizes sampled, the relative importance of new water in the generation of the event hydrograph decreases with increasing storm size. By explicitly routing direct channel precipitation through the Mink Brook catchment we find that the new water component of the event hydrograph can be almost entirely attributed to direct channel precipitation.

With the onset of precipitation, there is a rapid increase in stream discharge beyond that which can be explained by direct channel precipitation. The rapid increase in the contribution of subsurface flow to stream discharge requires a mechanism for rapidly increasing the fluid pressures at the base of the unsaturated zone. We suggest that kinematic flow in the unsaturated zone is consistent with our observations.

The excellent agreement between the observed and simulated contributions of direct channel precipitation to the event hydrograph highlights the ability of DEM-based numerical stream flow routing methodologies to quantify accurately direct channel contributions to an event hydrograph. This suggests that DEM-based numerical stream flow routing models can be used to predict the contribution of direct channel precipitation to stream flow when it cannot be determined isotopically, i.e. in catchments with significant saturation overland flow and/or catchments with isotopically similar end members. This would allow for the dilution of chemical compounds due to direct channel precipitation to be accurately quantified, resulting in more accurate analyses of stream chemical concentration versus stream discharge variations during storm events.

## Acknowledgements

Support for this work comes from the National Science Foundation grants ATM-9628759, EAR-9903281 and EAR-9814121.

## References

Bazemore, D.E., Eshleman, K.N., Hollenbeck, K.J., 1994. The role of soil water in stormflow generation in a forested headwater catchment: synthesis of natural tracer and hydrometric evidence. J. Hydrol. 162, 47–75.

Beston, R.P., 1964. What is watershed runoff? J. Geophys. Res. 69, 1541–1551.

Beven, K., 1989. Interflow. In: Morel-Seytoux, H.J., (Ed.), Unsaturated Flow in Hydrologic Modeling, Kluwer, New York, pp. 191–218.

Beven, K.J., Germann, P.F., 1982. Macropores and water flow in soils. Water Resour. Res. 18, 1311–1325.

Brammer, D.D., McDonnell, J.J., 1996. An evolving perceptual model of hillslope flow at the Maimai catchment. In: Anderson, M.G., Brooks, S.M. (Eds.), Advances in Hillslope Hydrology, Wiley, New York, pp. 35–60.

Bras, R.L., 1990. Hydrology: An Introduction to Hydrologic Science, Addison-Wesley, New York.

Brown, V.A., McDonnell, J.J., Burns, D.A., Kendall, C., 1999. The role of event water, a rapid shallow flow component, and catchment size in summer stormflow. J. Hydrol. 217, 171–190.

Charbeneau, R.J., 1984. Kinematic models for soil moisture and solute transport. Water Resour. Res. 20, 699–706.

Clow, D.W., Sueker, J.K., 2000. Relations between basic characteristics and stream water chemistry in alpine/subalpine basins in Rocky Mountain National Park, Colorado. Water Resour. Res. 36, 49–61.

Colbeck, S.C., 1972. A theory of water percolation in snow. J. Glaciol. 11, 369–385.

Dunne, T., Black, R.D., 1970. Partial area contributions to storm runoff in a small New England catchment. Water Resour. Res. 6, 1269–1311.

Dunne, T., Leopold, L.B., 1978. Water in Environmental Planning, Freeman, New York.

Eagleson, P.S., 1970. Dynamic Hydrology, McGraw-Hill, New York.

Elsenbeer, H., West, H., Bonell, M., 1994. Hydrologic pathways and stormflow hydrochemistry at South Creek, northeast Queensland. J. Hydrol. 162, 1–21.

Freeze, R.A., 1974. Streamflow generation. Rev. Geophys. Space Phys. 12, 627–647.

Freeze, R.A., Cherry, J.A., 1979. Groundwater, Prentice-Hall, Engelwood Cliffs, NJ.

Genereux, D.P., Hooper, R.P., 1998. Oxygen and hydrogen isotopes in rainfall-runoff studies. In: Kendall, C., McDonnell, J.J. (Eds.), Isotope Tracers in Catchment Hydrology, Elsevier, New York, pp. 319–346.

Hewlett, J.D., Hibbert, A.R., 1967. Factors affecting the response of small watersheds to precipitation in humid areas. In: Sopper, W.E., Lull, H.W. (Eds.), Proceedings of the International Symposium on Forest Hydrology, Pergamon, New York, pp. 275–290.

Hibberd, S., 1984. A model for pollutant concentrations during snow-melt.. J. Glaciol. 30, 58–65.

Hoggon, D.H., 1997. Computer-Assisted Floodplain Hydrology and Hydraulics, McGraw-Hill, New York.

Hooper, R.P., Christophersen, N., Peters, N.E., 1990. Modelling streamwater chemistry as a mixture of soilwater end-members—A application to the Panola Mountain catchment, Georgia, USA. J. Hydrol. 116, 321–343.

Horton, R.E., 1933. The role of infiltration in the hydrologic cycle. Trans., Am. Geophys. Union 14, 446–460.

Hursch, C.R., 1936. Storm water and absorption: dicussion of terms with definitions: report of the committee on absorption and transpiration. Trans. Am. Geophys. Union 17, 301–302.

IAEA, 1981. Stable Isotope Hydrology: Deuterium and Oxygen-18 in the Water Cycle, Technical Reports Series No. 210, International Atomic Energy Agency, Vienna.

Jenkins, A., Ferrier, R.C., Harriman, R., Ogunkkoya, Y.O., 1994. A case study in catchment hydrochemistry: conflicting interpretations from hydrological and chemical observations. Hydrol. Process. 8, 335–349.

Kirchner, W.J., Feng, X., Neal, C., 2000. Fractal stream chemistry and its implications for contaminant transport in catchments. Nature 403, 524–527.

Langmuir, D., 1997. Aqueous Environmental Geochemistry, Prentice-Hall, Upper Saddle River, NJ.

McCuen, R., 1998. Hydrologic Analysis and Design, Prentice Hall, Upper Saddle River, NJ.

McDonnell, J.J., 1990. A rationale for old water discharge through macropores in a steep, humid catchment. Water Resour. Res. 26, 2821–2832.

McDonnell, J., Bonell, M., Stewart, M.K., Pearce, A.J., 1990. Deuterium variations in storm rainfall: implications for stream hydrograph separation. Water Resour. Res. 26, 455–458.

Mullholland, P.J., 1993. Hydrometric and stream chemistry evidence of three storm flow paths in Walker Branch Watershed. J. Hydrol. 151, 291–316.

Mulholland, P.J., Wilson, G.V., Jardine, P.M., 1990. Hydrogeochemical response of a forested watershed to storms: effects of preferential flow along shallow and deep pathways. Water Resour. Res. 26, 3021–3036.

Ogden, C.B., Van Es, H.M., Schindelbeck, R.R., 1997. Miniature rain simulator for field measurement of soil infiltration. Soil Sci. Soc. Am. J. 61, 1041–1043.

Ross, D.S., Bartlett, R.J., Magoff, F.R., Walsh, G.J., 1994. Flow path studies in forested watersheds of headwater tributaries of Brush Brook, Vermount. Water Resour. Res. 30, 2611–2618.

Schnoor, J.L., 1996. Environmental Modeling: Fate and Transport of Pollutants in Water, Air, and Soil, Wiley, New York.

Sueker, J.K., Ryan, J.N., Kendall, C., Jarrett, R.D., 2000. Determination of hydrologic pathways during snowmelt for alpine/subalpine basins, Rocky Mountain National Park, Colorado. Water Resour. Res. 36, 63–75.

Tindall, J.A., Kunkel, J.R., 1999. Unsaturated Zone Hydrology for Scientists and Engineers, Prentice Hall, Upper Saddle River, NJ.

Torres, R., Dietrich, W.E., Montgomery, D.R., Anderson, S.P., Loague, K., 1998. Unsaturated zone processes and the hydrologic response of a steep, unchanneled catchment. Water Resour. Res. 34, 1865–1879.